의학 박사 학위논문

Identification of the pathophysiology of cardiac microvasculopathy in diabetes mellitus and its effect on the remodeling of coronary arteries

당뇨병성 심근 미세혈관병증 병태생리 규명과 관상동맥 재형성에 미치는 영향

2018년 2월

서울대학교 대학원

의학과 분자유전체 전공

박 진 주

Identification of the pathophysiology of cardiac microvasculopathy in diabetes

mellitus and its effect on the remodeling of coronary arteries

지도교수 김 명 아

이 논문을 의학박사 학위논문으로 제출함

2017년 10월

서울대학교 대학원

의학과 분자유전체 전공

박 진 주

박 진 주 의 의학박사 학위논문을 인준함

2017년 12월

위 원 장 _____ (인)

부 위 원 장 _____ (인)

위 원 _____ (인)

위 원 _____ (인)

위 원 _____ (인)

Abstract

Identification of the pathophysiology of cardiac microvasculopathy in diabetes mellitus and its effect on the remodeling of coronary arteries

Jin Joo Park

Laboratory of Molecular Genetics and Genomic

The Graduate School

Seoul National University

Background

Diabetes mellitus (DM) causes macro- and microvasculopathy. Data on cardiac microvascular changes in large animals are scarce. We sought to determine the effect of DM on macro- and microvascular changes in diabetic pigs and humans.

Methods

Eight domestic pigs (4 with type I DM and 4 controls) underwent coronary angiography with optical coherent tomography (OCT; at baseline and 1 and 2 months), coronary CT angiography (CCTA), cardiac magnet resonance (CMR) imaging, and histologic examination.

Results

The diabetic pigs had more irregular capillaries with acellular capillaries and a smaller capillary diameter (11.7±0.33 ㎛ vs. 13.5±0.53 ㎛, P<0.001) than those of the control pigs. The OCT showed no significant epicardial stenosis in either group; however diabetic pigs had a greater intima-media thickness. CMR results showed that diabetic pigs had a lower relative upslope at rest (31.3±5.9 vs. 37.9±8.1, P = 0.011) and during stress (18.0±3.0 vs. 21.6±2.8, P = 0.007) than the control pigs, implying decreased myocardial perfusion.

Among the 79 patients with ST elevation myocardial infarction, 25 had DM and they had lower myocardial perfusion on CMR as well.

Conclusions

DM causes increase in intima-media thickness and microvascular remodeling leading to a decrease in myocardial perfusion in large animals at a very early stage of the disease course. Early and effective interventions are necessary to interrupt the progression of vascular complications in diabetic patients.

Key words: diabetes mellitus; cardiac microvasculopathy, capillary changes, myocardial perfusion; heart MRI, coronary angiography, optical computer tomography

Student ID: 2011-30599

CONTENTS

LIST OF FIGURES

LIST OF TABLES

Introduction

Diabetes mellitus (DM) is a well-known risk factor for coronary artery disease and coronary artery disease is common in diabetic patients. The age-adjusted incidence of coronary artery disease was four times greater in diabetic patients than those without DM(1), and coronary artery disease is the leading cause of death in diabetic patients. Diabetic patients have cardiovascular complications at an earlier age, often have multi-vessel disease, and silent ischemia, and, most importantly, worse clinical outcomes despite revascularization (2). In patients with acute myocardial infarction, DM is a strong risk factor for death, recurrent infarction, and heart failure (3).

DM causes chronic vascular disease in both macro- and microvascular system, eventually leading to multi-organ dysfunction. The major microvascular complications include nephropathy, retinopathy, and neuropathy, and indeed, DM is the leading cause of blindness (12.5%) and end-stage renal disease. Regarding macrovascular changes, DM is associated with accelerated atherosclerosis, resulting in premature coronary, peripheral, and cerebrovascular disease. DM is associated 2-4 fold and 2.5 fold increased risk for cardiovascular mortality and stroke, respectively. It is of note that more than 65% of mortality in diabetic patients was attributed to cardiovascular disease.

Altered glucose homeostasis seems to play a major role in the initiation of diabetic vasculopathy. As a consequence of impaired glucose homeostasis,

metabolic, humoral, and hemodynamic disturbance contribute to the initiation and progression of vasculopathy in diabetic patients (4). Suggested mechanisms include hyperglycemia-induced apoptosis or structural changes in vascular endothelial cells and cardiomyocytes through inflammation, oxidative stress, glycated products, or protein kinase C activation (5,6). Recently, we found a novel mechanism where abnormal intercellular signaling in endothelial cells decreased the capillary diameter and induced microvascular rarefaction in diabetic conditions in a human in-vitro model of angiogenesis and in the retina, heart, skeletal muscle, and kidney of mice(7,8). The microvascular changes in DM has not been evaluated in a large animal model or human. The diagnosis of coronary microvasculopathy in patients with DM is challenging because macrovascular changes often coexist and the histologic examination of microvessels is not feasible.

Regarding heart, the effect of DM on coronary macrovasculature, i.e. epicardial coronary artery, has been extensively studied; however, data on coronary microvasculopathy are scarce. Previous studies reported “paradoxical” absence of significant stenosis in epicardial arteries in patients with significant ischemic symptoms and positive exercise test (9-11), implying the existence of microvasculopathy leading to significant myocardial ischemia without significant macrovasculopathy.

It is unknown, whether (i) the microvasculopathy exists in all diabetic patients, (ii) it represents a pre-condition or precursor to macrovasculopathy, (iii) it is a risk factor for adverse clinical outcome, (iv) or it is a reversible process that

responds to intensive therapy.

Functional and structural abnormalities of the coronary microcirculation are often observed in diabetic patients with normal coronary arteries (12-14). The coronary microcirculation can be functionally evaluated by measurement of coronary flow reserve (CFR). CFR is the ratio between hyperemic and resting coronary flow, and in the absence of significant stenosis of the epicardial coronary arteries, the reduction of CFR represents coronary microvascular dysfunction (15). A reduction of CFR was demonstrated by different techniques in diabetic patients without coronary artery stenosis (16). Possible mechanisms for the reduced GFR in diabetic patients include hyperglycemia (17), insulin resistance (18), endothelial dysfunction (19) and increased cardiac sympathetic activity (20); nonetheless, the mechanisms are not fully understood.

According to fluid hemodynamic, at a constant pressure, the flow is determined by the resistance. In coronary circulation, coronary flow will be determined by microvascular resistance and structures. Furthermore, the structure of the artery wall is sensitive to the hemodynamic forces and vascular remodeling is a homeostatic response to changes in flow and circumferential stretch to maintain or restore normal shear stress and wall (21). A reduction in blood flow causes a decrease in vessel diameter (22).

We hypothesized that (i) DM would cause alterations in capillary structure, (ii) causing an increase in microvascular resistance and finally(iii) leading to

decreased myocardial perfusion. We sought to determine the effect of DM on macro- and microvasculature in heart. For this purpose, we created a diabetic pig model and intended to exam the anatomic and functional changes in the heart vessel. Here, we performed the state-of-the-art diagnostic procedures including coronary angiography (CAG), optical coherence tomography (OCT), coronary computed tomography angiography (CCTA) and cardiac magnet resonance (CMR) imaging, amongst others. In addition, we also validated our findings in diabetic patients using cardiac magnet resonance imaging.

Materials and Methods

Study design and animals

A total of 8 domestic female pigs weighing between 20 and 25 kg were used for the experiment. DM was induced in six pigs, whereas the remaining six pigs served as healthy controls. The pigs underwent coronary angiography with OCT at 1 and 2 months and CMR and CCTA at 2 months. After invasive and non-invasive imaging, the pigs were sacrificed for histologic analyses.

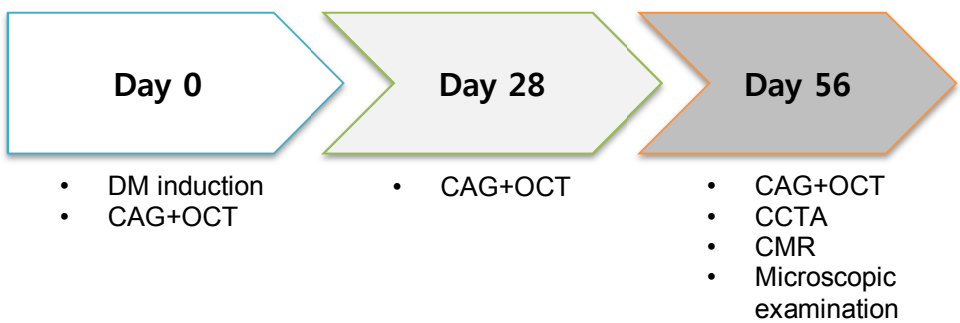

Figure 1 Study flow

Induction of diabetes mellitus

Streptozotocin has been widely used to induce long-lasting DM in animals instead of pancreatectomy in pigs without detrimental side effects (23,24). To induce type I DM, streptozotocin was administered by interaperitoneal injection at a dose of 150 mg/kg. Consecutive measurements of serum glucose were performed, before and up to 16 hours after injection of streptozotocin, and every 2 weeks thereafter. Sustaining blood glucose level > 250 mg/dL was considered as having DM. If blood glucose exceeds 400 mg/dL, 4 to 8 units of insulin was injected to avoid acute complications such as diabetic ketoacidosis or hyperosmolar coma.

The current study protocol was approved by Institutional Animal Care and Use Committee of Seoul National University Bundang Hosptial (IACUC No. BA1111-093/071-01).

Anesthesia of the animals

The anesthesia of the animals was initiated by intramuscular injection of anesthetic medications. First, the pigs received a premedication with atropine sulfate (0.5 mg/kg), and then Zoletil (4-6 mg/kg) and Xylazine (4.4 mg/kg) via intramuscular injection. After endotracheal intubation, the anesthesia was maintained with 70% N_2O and isoflurane (1-2%) in oxygen (2 L/min) using an anesthesia ventilator. Adequate anesthesia was confirmed by the absence of a limb withdrawal reflex.

Surface electrocardiogram (ECG) and blood pressures were recorded, and capnometer and pulse-oxymeter were applied to monitor the effective ventilation throughout the procedure. An experienced veterinarian performed the induction, maintenance, and end of the anesthesia.

Euthanasia of the animal

After completion of the experiment of each pig, the pigs were killed. Induction of intravenous anesthesia with atropine sulfate (0.5 mg/kg) and Zoletil+Xylazine (4-6 mg/kg + 4.4 mg/kg) was performed, followed by an injection of potassium chloride. After confirmation of cardiac arrest, the organs were harvested.

Coronary angiogram and optical coherence tomography

Coronary angiogram was performed with standard technique. The animals were given aspirin (300 mg) and clopidogrel (300 mg) 1 day before the procedure. Under general anesthesia, 5-French arterial sheath was positioned to the femoral artery using the Seldinger Technique. Under fluoroscopic guidance, 5-French Judkin Left 3.5 and Judkin Right 3.5 guiding catheters were positioned in both coronary ostia. After the intracoronary administration of nitroglycerin (200 μg), coronary angiography was performed in the anterio-posterior view and was recorded by cineradiography. Five thousand units of unfractionated heparin was

administered intra-coronary to prevent thrombus formation.

Optical coherence tomography

OCT provides opportunities to perform a sophisticated analysis of coronary artery, because it generates ultra-high resolution cross-sectional images of tissue layers using infrared back-reflected light. The resolution of OCT is 10 to 30 times higher than conventional intravascular ultrasound, enabling quantification at micron-scale level.

The OCT system consisted of an optical fiber, a proximal low-pressure occlusion balloon catheter (Helios™ Goodman, Advantec Vascular Corp™, Sunnyvale, CA) and an OCT system mobile cart containing the optical imaging engine and computer for signal acquisition, analysis and image reconstruction (M2CV OCT Imaging System, LightLab, Westford, MA).

After intracoronary administering 5000 units of unfractionated heparin, left anterior descending artery (LAD) and circumflex artery (LCX) were wired with 0.014 inch Runthrough guide wire (Terumo, Japan). The guide wire was positioned distal segment of each coronary artery. A short nose balloon (4×2 mm^2), compatible with large 6-French guiding catheters (0.071" inner diameter) is advanced to the mid segment of the artery over the Runthrough angioplasty guide wire (0.014"). The guide wire is then replaced by the OCT ImageWire™ and the occlusion balloon was pulled-back and was positioned in a mid-segment of the

artery. Inflation was performed gently up to 0.4–0.7 atmosphere by a dedicated inflation device. During the scanning of the artery the use of balloon occlusion catheter with constant hand flush through the distal tip was performed to avoid blood interference occurs and to acquire the best possible image. Heparinized normal saline was injected through the end-hole of the occlusion balloon catheter to minimize arrhythmias. Infusion should start a few seconds before balloon inflation to get images clean from blood contamination when recording starts.

The vessel segments were imaged using an automated pull-back (1.0 mm/sec) from distal to proximal segments. Images were acquired at 15.4 frames/sec and displayed in a real-time 2D array at different transverse positions.

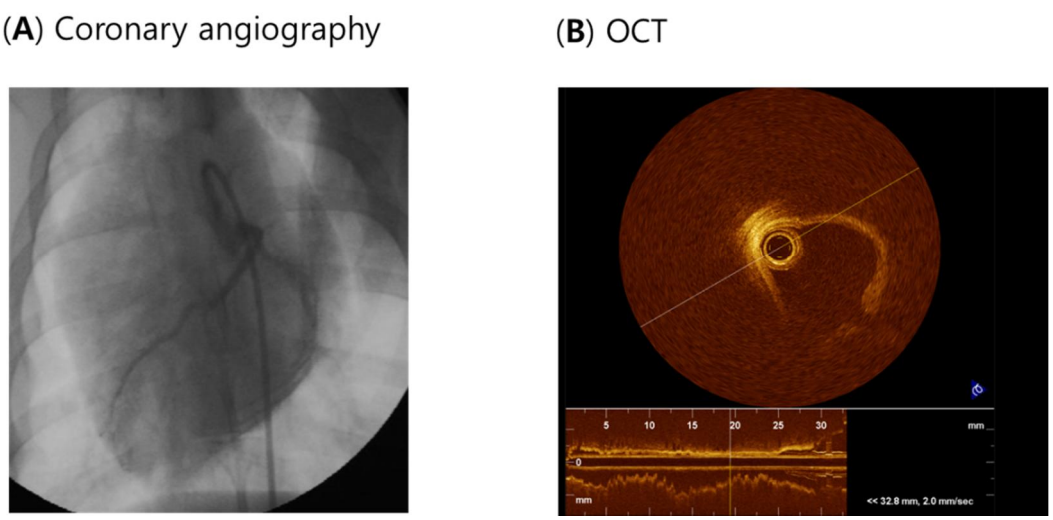

Figure 2 Coronary angiography and OCT

Coronary computed tomography angiography

Eight pigs underwent CCTA with a 64-slice multi-detector CT (MDCT) scanner (Brilliance 64; Philips Medical Systems, Best, The Netherlands) in the prone-position. Prior to CCTA, all animals with a baseline heart rate > 70 beats/min received 10 to 30 mg of intravenous esmolol (Jeil Pharm, Seoul, Korea). CCTA was performed with a 64 x 0.625 mm section collimation, 420-ms rotation time, 120-kV tube voltage, and 800-mA tube current. During CCTA acquisition, a bolus of 80 ml iomeprol (Iomeron 400, Bracco, Milan, Italy) was injected intravenously (4 ml/s). The animals' ECG was simultaneously recorded to allow for retrospective segmental data reconstruction. Images were initially reconstructed at the mid-diastolic phase (75% of R-R interval) of the cardiac cycle. Compartment analysis was performed by using the cardiac CT viewer tool of the workstation (IntelliSpace Portal ISP, Version 8.0; Philips). Center lines were rotated to the sagittal plane to acquire suitable short-axis pig heart image. Hounsfield units (HU) of region of interest were measured using the dedicated software in the 16 segments (American Heart Association model, true apex not imaged) of the heart, ascending and descending aorta, and left ventricular cavity in 2 or 3 phases of the heart cycle. We calculated the ratio of HU of the myocardial segments to the averaged HU of the aorta and LV cavity.

Cardiac magnet resonance imaging and perfusion

All CMR studies were performed using a 1.5 T MRI scanner (Siemens Avanto, Erlangen, Germany or Intera CV release 10; Philips Medical Systems, Best, Netherlands) with a phased array cardiac coil. Hemodynamic parameters, oxygen saturation and lead vector ECG rhythm will be continuously monitored throughout the exam. Following image localizers, ventricular long and short axis cine images will be acquired in end expiration with retrospectively ECG-gated steady-state free precession sequences (image matrix 128 × 128, read field of view (FOV) 340 mm, phase FOV 75–100% of the FOV read, echo time 1.12 ms, flip angle 70°) with slice thickness of 8 mm and intersection gaps of 12-15 mm.

Adenosine (Adenoscan®, Sanofi-Synthelabo) was infused at 140 μg/kg/min, via a 20-gauge cannula sited into a vein in the ear using a syringe pump (Graseby® 3500). Adenosine was infused for a minimum of 6 min before acquiring stress images. Scans were supervised by an MRI trained clinician with access to immediate resuscitation facilities.

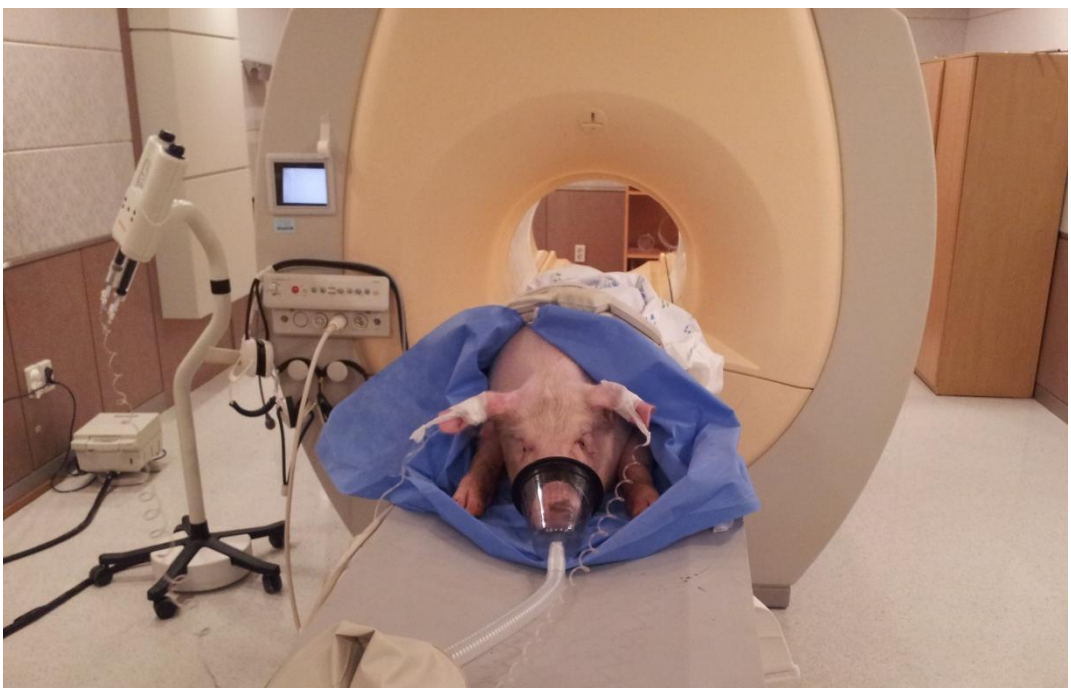

Figure 3 Pig undergoing cardiac magnet resonance imaging

Pigs underwent pharmacological stress and rest perfusion. Electrocardiographic gating and triggering will be performed using the vector cardiographic method. Fast survey images were acquired to determine the true

short axis of the left ventricle. After the acquisition of rest cine scans in the standard views, adenosine was infused at a dose of 140 μg/kg/min for up to 6 minutes. During the adenosine infusion, electrocardiographic activity was continuously monitored, and blood pressure and heart rate measurements were obtained every minute. Within the last minute of infusion, the adenosine stress MR perfusion scan were performed to visualize the 3 short-axis slices of 8 mm section thickness using 40 dynamic acquisitions. During the inspiratory phase of the second breath, a bolus of gadodiamide (Omniscan; GE healthcare, U.S.A) was injected, using a power injector (Spectris; Medrad, Indianola, PA), into vein at a dose of 0.1 mmol per kilogram of body weight and an injection rate of 4 ml/s and followed by a 20 mL-saline flush. Stress perfusion MR images was obtained with a gradient-echo sequence by using saturation-recovery steady-state free precession (SR-SSFP). After 15-25 minutes, identical MR perfusion scan at rest will be continued to allow adequate clearance of the first bolus of the contrast agent.

Data were analyzed using a dedicated software (QMass, Medis, the Netherlands). For functional analysis, left ventricle (LV) contours were drawn manually on the short-axis images at the end of diastole and of systole, and the contours were propagated automatically to other images for the rest of the cardiac cycle. Then, manual correction of the automatically rendered endocardial and epicardial contours was performed for all datasets, and papillary muscles as well as myocardial trabeculations were included in the ventricular cavity.

First-pass perfusion images at stress and rest states were analyzed

semiquantitatively. Subendocardial and subepicardial borders were positioned on each slice on a frame with high contrast between the LV cavity and the myocardium. The borders were propagated automatically onto all frames. An interactive correction was done if necessary. The LV cavity region of interest was adjusted manually so that it would include the region of maximal signal intensity within the cavity and exclude papillary muscle. An American Heart Association 16-segment model was used (true apex not imaged), resulting in a total of 32 segments per patient (16 for the stress examination and 16 for the resting examination). Signal intensity–time curves were generated for all segments and the maximum upslope of the LV myocardium divided by the maximum upslope of the LV cavity. The myocardial perfusion reserve index (MPRI) was calculated as the ratio of the segmental upslope values during adenosine stress and rest [MPRI = relative upslope at stress(SRU)/relative upslope at rest(RRU)].

Immunofluorescence staining and confocal microscopic analysis

After euthanasia of the pigs, the coronary arteries were perfused with phosphate-buffered saline (PBS) and 2% paraformaldehyde (PFA) in PBS at room temperature. The isolated tissues were embedded in an optimal cutting temperature compound (OCT; Tissue-Tek, USA) and stored in a -80°C deep freezer. Frozen sagittal sections were cut into 25 to 30 μm slices using a cryostat (HM 550 MP,

Microm; Walldorf, Germany). The sections were fixed with 4% PFA in PBS for 10 min and permeabilized with 10% fetal bovine serum (FBS) and 0.5% Triton-X100 in PBS for 4 to 6 hours. We incubated the slices with tetramethyl rhodamine isothiocyanate (TRITC)-conjugated Bandeiraea simplicifolia (BS)1-lectin (Sigma Aldrich) and FITC-conjugated alpha smooth muscle actin (Sigma Aldrich) overnight at 4°C. We also stained the slices overnight at 4°C with specific primary antibody, anti-VE-cadherin (Santa Cruz Biotechnology, Santa Cruz, CA, USA), followed by incubation with fluorescent-tagged secondary antibodies (Invitrogen, Carlsbad, CA, USA) overnight at 4°C. The images were acquired by a confocal laser scanning microscope system (LSM 710, Carl Zeiss AG, Oberkochen, Germany) and processed with Zen2008 (Zeiss) and ImageJ (NIH, MD, USA) software. A water- or oil-immersion objective (40× or 63×, 1.4 numerical aperture) with a pinhole set for a section thickness of 0.8 to 1.2 µm (1 airy unit in each channel) was used. To visualize the three-dimensional reconstructed image, a Z-stack of 20-µm thickness was obtained. Diode 405 nm, Multi-Argon 488 nm, HeNe 543 nm, and HeNe 633 nm laser lines were selected and images were sequentially acquired using separate laser excitations to avoid cross-talk between different fluorophores.

Immunofluorescence quantification of microvasculopathy in

the myocardium

Images were generated for comparative analysis under identical conditions of light, contrast, and magnification. The capillary density and diameter were measured with ImageJ software (NIH, MD, USA). We directly evaluated the capillary diameter at various points of interest in z-stack images by measuring the width of the lectin-positive area perpendicular to the capillary length. Therefore, the capillary diameter in our data denotes the abluminal diameter of the capillary, not the luminal diameter.

Patients

We retrospectively enrolled patients with ST-segment elevation myocardial infarction (STEMI) who underwent CMR 5 to 7 days and 6 months after the onset of MI from January 2005 to November 2012. We then compared the myocardial perfusion in non-infarct segments between patients with and without DM. The study protocol was approved, and informed consent was waived by the Institutional Review Board (IRB no: B-1703-388-102).

Statistical Analysis

Continuous variables were expressed as mean ± SD or mean ± SE and categorical variables were presented as absolute numbers and proportions (%). Overall comparisons between groups were performed with the Student's t-test for continuous variables and the Chi-square or Fisher's exact test for categorical variables. To compare the MR perfusion, we applied the two-way analysis of variance (ANOVA) test. Analyses were performed with SPSS Version 22.0 (IBM Statistics, Armonk, NY) and R programming version 3.1.0 (The R Foundation for Statistical Computing, Vienna). A two-sided P-value < 0.05 was considered statistically significant.

Results

Microvascular changes

Heart:

We induced DM in pigs by intraperitoneal injection of streptotozocin, and after 2 months, the diabetic and non-diabetic pigs were killed, and their hearts harvested. There was no difference in pigs' weights between the groups on days 0 and 56.

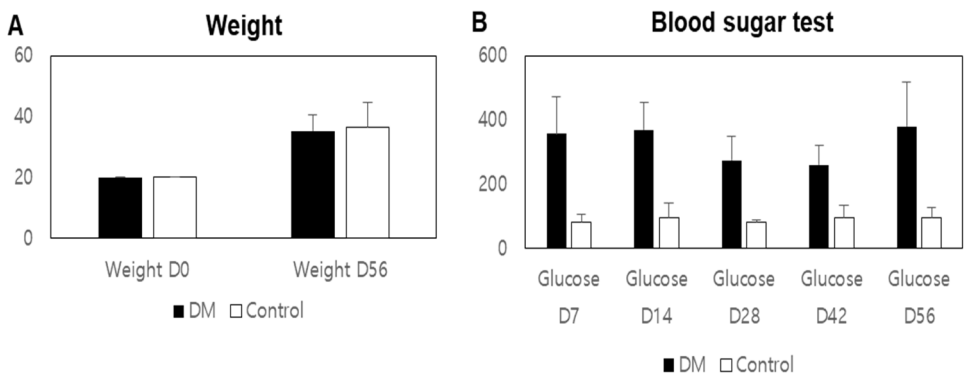

Figure 4 **(A) Weight of the pigs on day 0 and day 56 (B) The results of serum glucose tests of the pigs at different time points**

Both groups showed similar weight gain during the experiment. Blood glucose level in the diabetic pigs was significantly higher than that in the control pigs during the experiment.

For the evaluation of microvasculature, we first evaluated the capillary

anatomy. Considering different anatomy of the heart, we divided the heart in 6 segments, i.e. anterior, anterioseptal, inferoseptal, inferior, inferolateral, and anterolateral segment. In each segment, more than four measurements were performed, each for lengths, branching points, and diameter. In the confocal microscope, the capillaries in the diabetic pigs seemed much more irregular; the capillary diameter varied strongly with frequent acellular capillaries, so called string vessels. The capillaries showed disruption and their lengths were shorter.

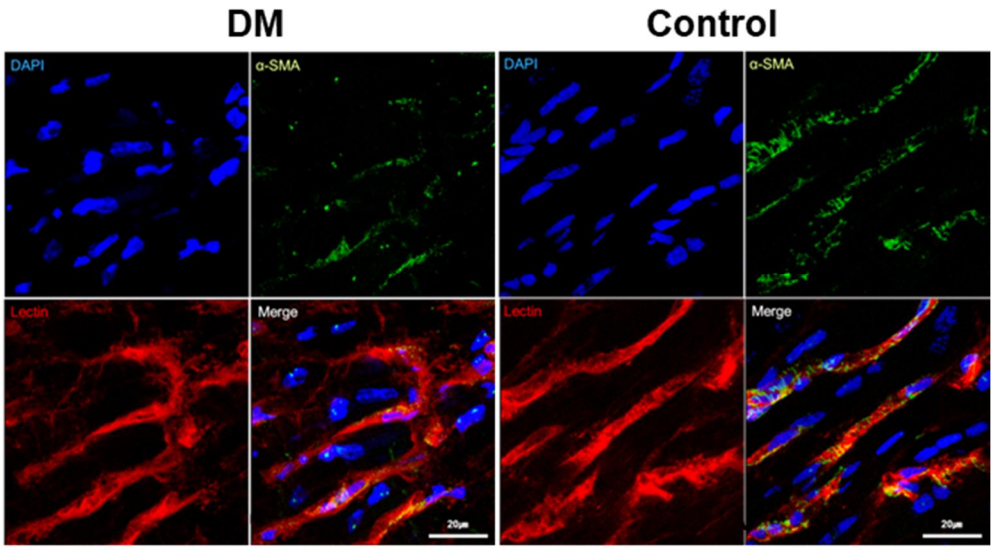

Figure 5 Myocardial capillaries of the diabetic and control pigs.

The two components of interest were the capillary density and diameter. Diabetic pigs had lower capillary density than the control pigs (24.6±9.6% vs. 32.3±8.5%, P = 0.019). Furthermore, diabetic pigs had a significantly smaller

capillary diameter (11.7 ± 0.33 ㎛ vs. 13.5 ± 0.53 ㎛, P = 0.00006) as we previously reported.

Table 1 Capillary anatomy in diabetic and control pigs

	Diabetes	Control	P-value
Capillary density (%)	24.6±9.6	32.3±8.5	0.019
Capillary diameter (㎛)	11.7±0.33	13.5±0.53	0.00006
Number of branching points	14.0±1.10	14.8±1.33	0.263

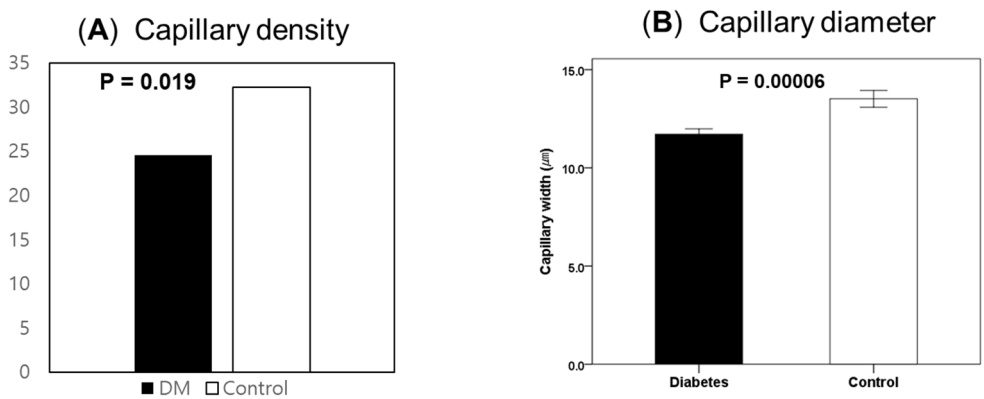

Figure 6 Quantification of the capillaries between diabetic and control pigs

We also found that VE-cadherin expression in the diabetic capillary was decreased and discontinued compared to that in the control.

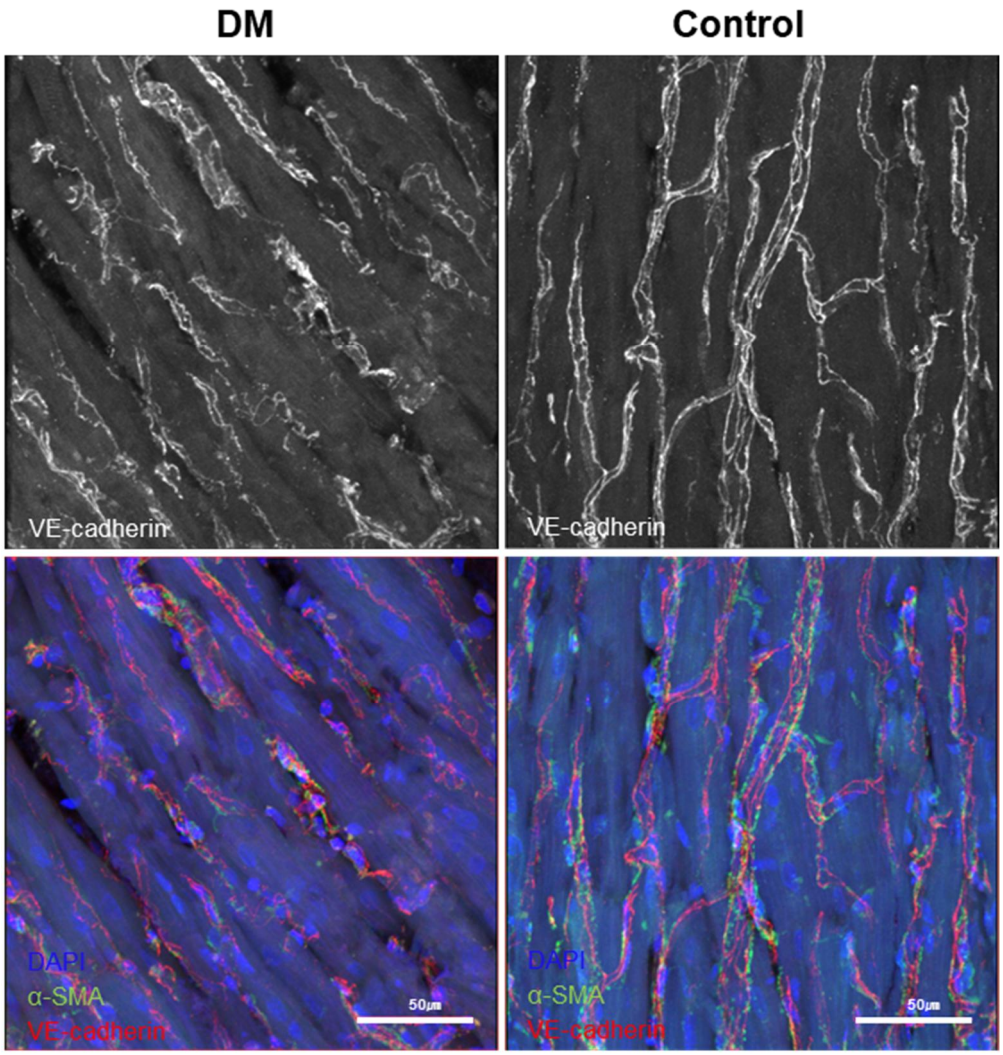

Figure 7 Capillary endothelial junction (VE-cadherin) in the diabetic and control pigs

Retina:

After harvesting of the eyes, the retina of the pigs was separated, and stained for the further analysis. Overall, diabetic pigs showed markedly decreased capillary in

the retina than control pigs, suggesting a probable rarefaction of the capillaries associated with DM.

The capillary anatomy was similar in the retina to those in the myocardium; diabetic pigs had smaller capillary diameter, whereas the branching points showed no difference.

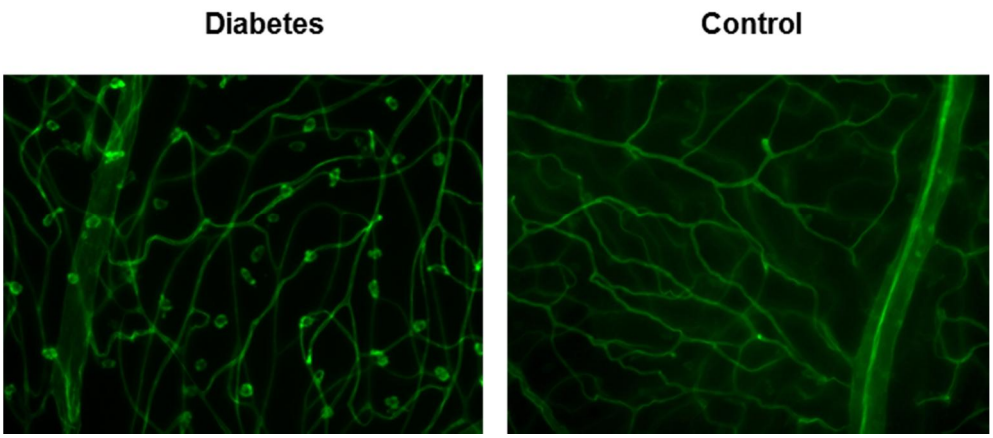

Figure 8 Capillary density and diameter in the retina of the diabetic and control pigs

Macrovascular changes:

Coronary angiography and optical coherent tomography

OCT enables accurate anatomic evaluation of coronary artery. We performed coronary angiography and OCT to evaluate the coronary anatomy of the pigs

accurately and to assess whether DM-induced macrovasculopathy can be observed.

According to the protocol, coronary angiography and OCT were performed at three time points: baseline, 1 month, and 2 months.

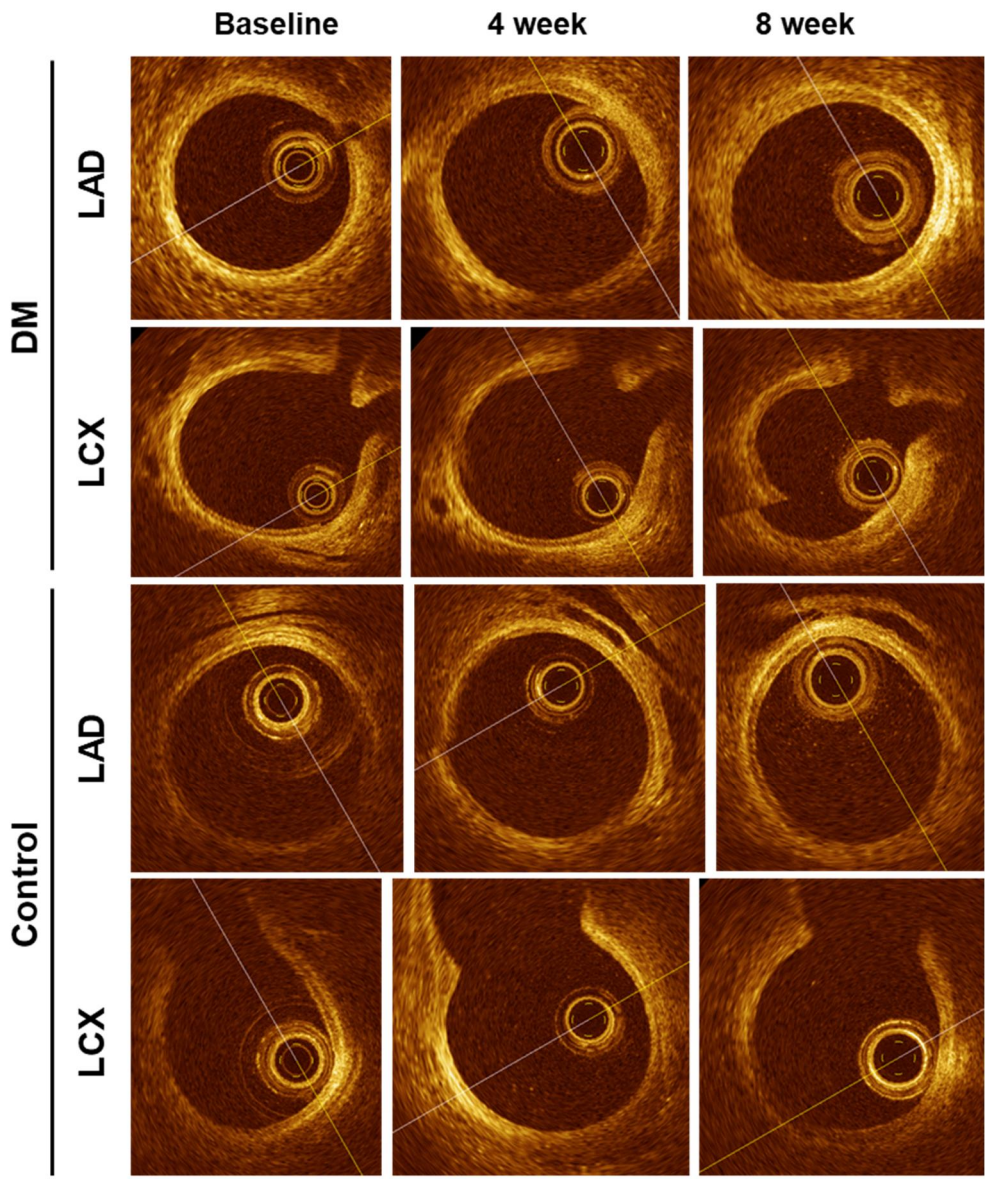

Figure 9 OCT images of the coronary arteries of diabetic and control pigs at

baseline, 4 weeks, and 8 weeks.

The size of the coronary artery of the pigs increased with their growth. There was no difference in the vessel size of the proximal LAD between diabetic and control pigs (at baseline 5.59 ± 0.60 mm vs. 5.68 ± 1.26 mm, P = 0.906; at 8 weeks: 7.31 ± 1.34 mm vs. 7.34 ± 1.47, P = 0.983). The lumen diameter of the proximal LAD did not differ (at baseline: 4.56 ± 0.43 mm vs. 4.72 ± 1.16 mm, P = 0.806; at 8 weeks: 5.45 ± 1.29 mm vs. 6.07 ± 1.22 mm, P = 0.582). However, diabetic pigs, but not the control pigs, showed a significant increase in intima-media thickness (IMT), a marker for atherosclerotic changes of a vessel, from baseline to 8 weeks. Consequently, diabetic pigs had a greater IMT than control pigs (at 4 weeks 1.50 ± 0.19 mm vs. 1.02 ± 0.17 mm, P = 0.019; at 8 weeks: 1.86 ± 0.30 mm vs. 1.27 ± 0.27 mm, P = 0.065). There was no hemodynamically significant stenosis in the epicardial coronary arteries in both groups.

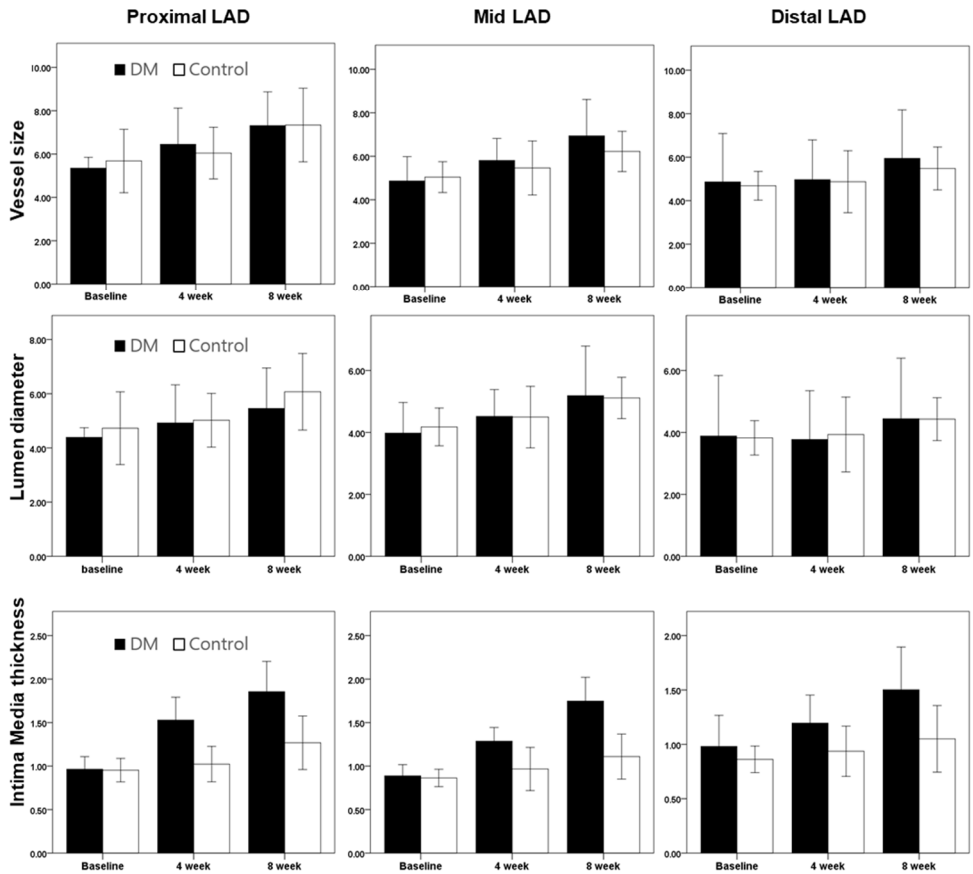

Figure 10 Vessel size, lumen diameter, and intima media thickness of the three segments of LAD at baseline, 4 weeks, and 8 weeks.

Myocardial perfusion analysis

Magnetic resonance perfusion

The myocardial perfusion by CMR at rest and during stress was measured in the sixteen myocardial segments in the diabetic and control pigs.

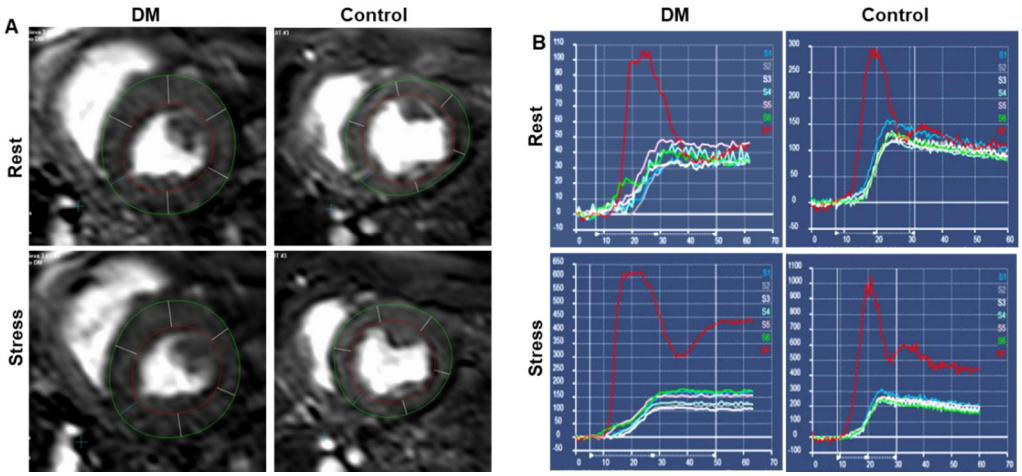

Figure 11 A) Representative figures measuring the myocardial perfusion in the 6 segments of the mid ventricle at rest and under adenosine stress. B) Representative figures of the measured myocardial perfusion graphs.

Red line = signal intensity-time curve of the left ventricular cavity; Cyan lines = signal intensity-time curve of the 6 midventricular myocardial segments

Diabetic pigs had lower mean values of relative upslope at rest (RRU) and relative upslope at stress (SRU) in most segments. However, MPRI showed no difference. We calculated estimated mean of the RRU, SRU, and MPRI of the 16 segments.

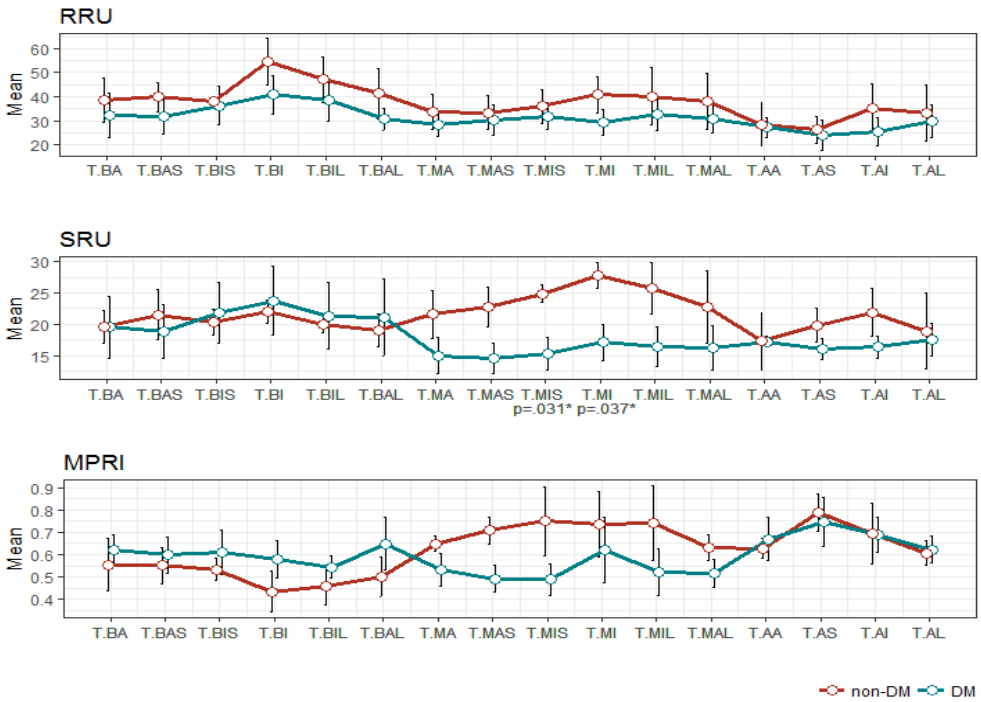

Figure 12 Mean values of the RRU, SRU and MPRI of the 16 myocardial segments.

BA = basal anterior; BAS = basal anteroseptal; BIS = basal inferoseptal; BI = basal inferior; BIL = basal inferolateral; BAL = basal anterolateral; MA = mid anterior; MAS = mid anteroseptal; MIS = mid inferoseptal; MI = mid inferior; MIL = mid inferolateral; MAL = mid anterolateral; AA = apical anterior; AS = apical septal; AI = apical inferior; AL = apical lateral. Error bars = SD.

Diabetic pigs had significantly lower RRU than control pigs (31.3 ± 5.9 vs. 37.9 ± 8.1, P = 0.011). Diabetic pigs also had lower SRU for myocardial perfusion

than control pigs (18.0 ± 3.0 vs. 21.6 ± 2.8, P = 0.007). However, there was no difference in MPRI between diabetic and control pigs (0.59 ± 0.05 vs. 0.62 ± 0.08, P = 0.380).

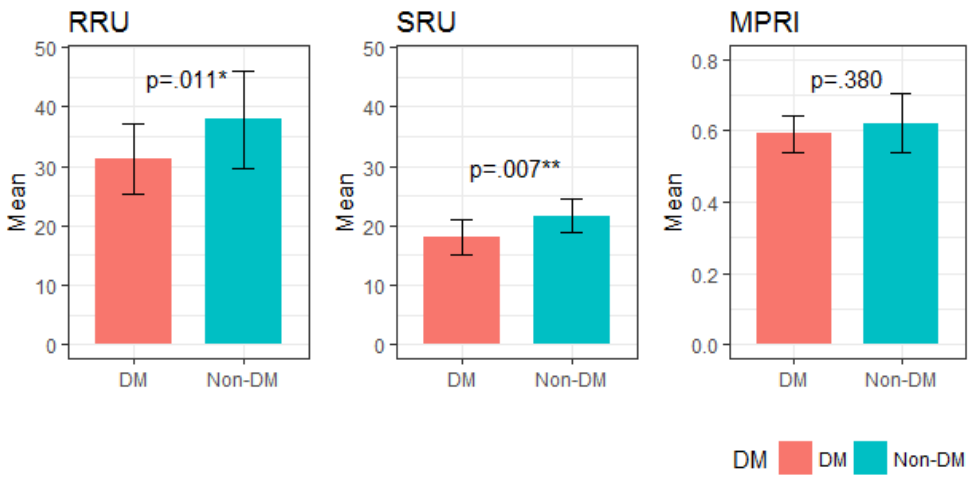

Figure 13 Estimated mean of RRU, SRU, and MPRI in diabetic and control pigs. P value by two-way ANOVA

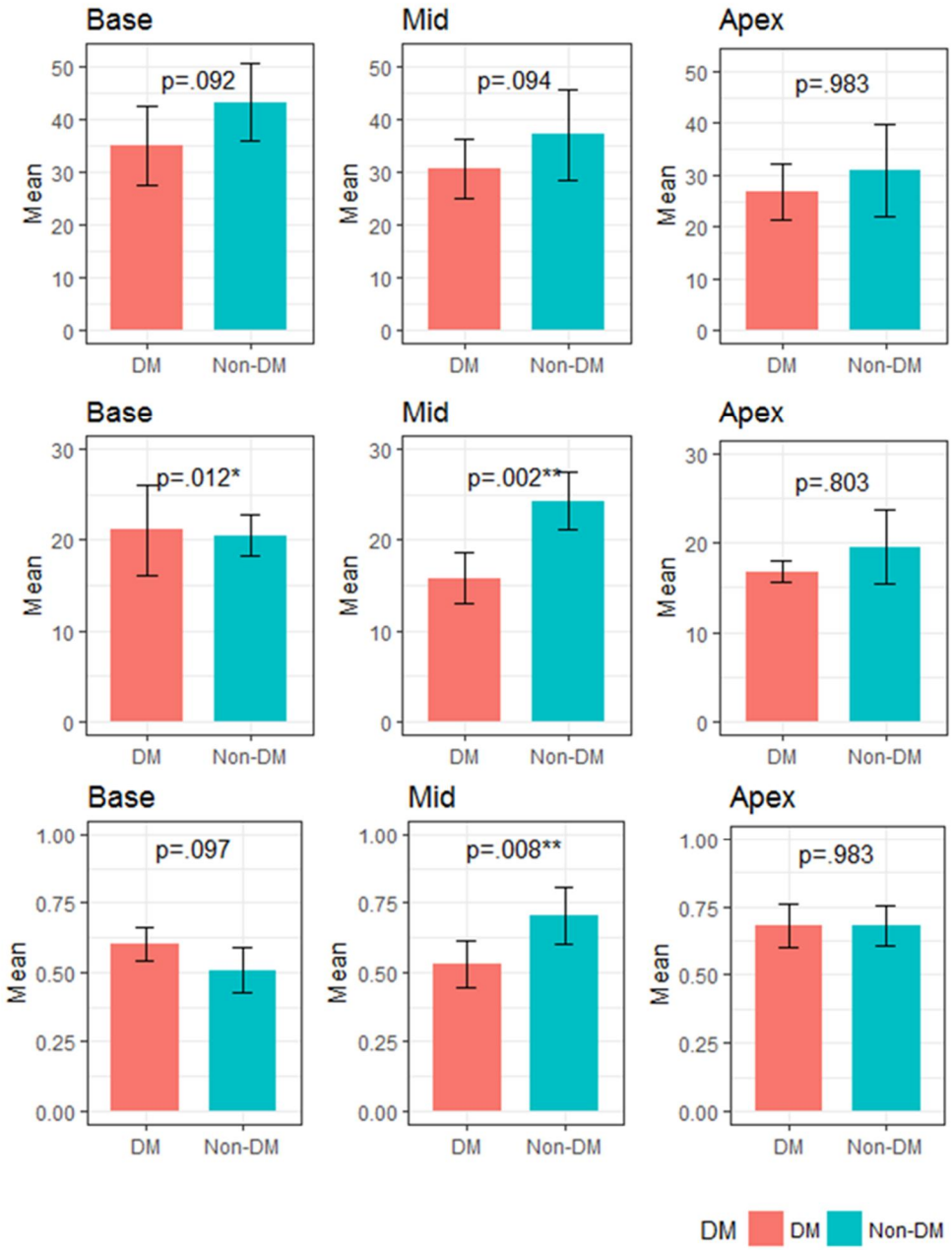

Figure 14 **Estimated mean of RRU, SRU, and MPRI in diabetic and control pigs** stratified by base, mid and apex**.**

P value according to base, mid and apical segments.

When stratifying the heart according to base, mid and apical segments, in the mid segments the MPRI was significantly lower in diabetic pigs (P=0.008).

CT angiography

Myocardial signal intensity (SI) in the arterial phase of the CT angiography represents myocardial texture and the amount of contrast in the myocardial microvessels. Therefore, we measured the Hounsfield unit of 16 segments of the LV in the arterial phases and compared them to those of the aorta.

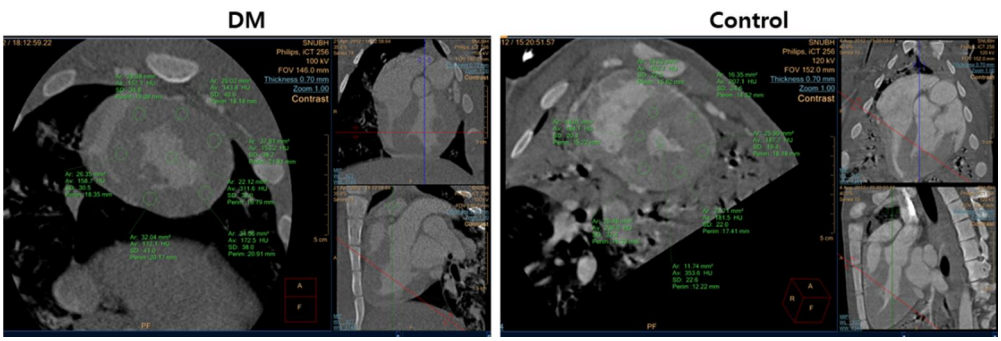

Figure 15 Quantification of contrast-enhanced myocardial signal intensity (SI) in the arterial phases of CT angiography. Regions of interest were drawn in the six segments of mid ventricle in the diabetic and control pigs.

CT perfusion showed similar results in that estimated mean of ratio of myocardial SI to aortic SI was significantly lower in the diabetic pigs compared to the control pigs (0.43 ± 0.05 vs. 0.48 ± 0.02, P < 0.001).

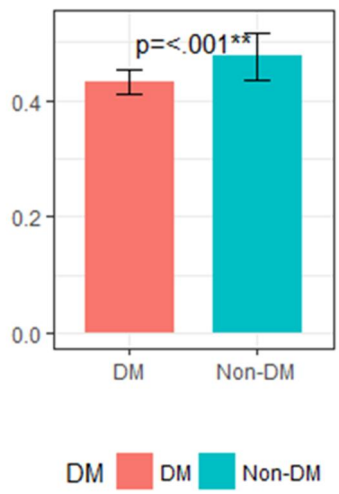

Figure 16 Estimated mean of ratio of myocardial SI to aortic SI. P value by two-way ANOVA

We further stratified the pigs according to the location, i.e. base, mid, and apex. Diabetic pigs had numerically lower estimated mean of ratio of myocardial SI to aortic SI perfusion across base, mid and apex.

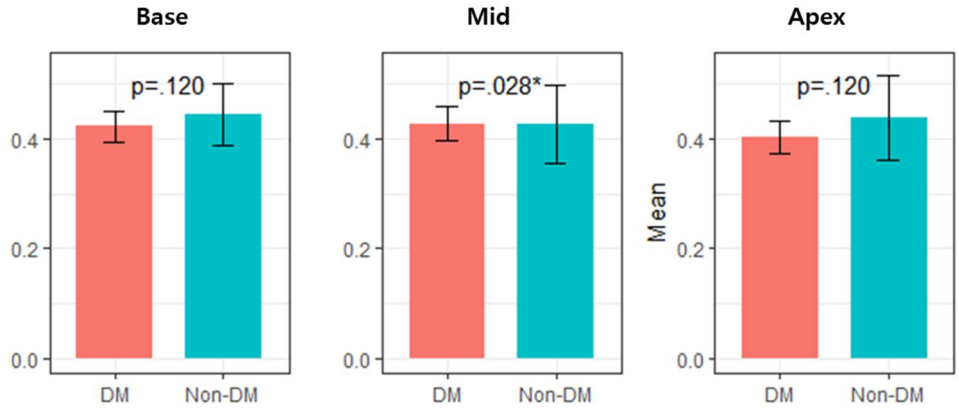

Figure 17 Estimated mean of ratio of myocardial SI to aortic SI according to the location. P value by two-way ANOVA

Myocardial flow analysis in patients with myocardial infarction

Next, we aimed to evaluate whether decreased myocardial perfusion is also observed in human with DM. For this purpose, we retrospectively enrolled 79 patients with ST-elevation myocardial infraction (STEMI) who underwent CMR. Baseline characteristics, MI-culprit lesions, baseline LV function, and infarct size did not differ between the patients with and without DM.

Table 2 Clinical characteristics and cardiac magnet resonance data of patients with myocardial infarction.

	Overall (n=79)	No DM (n=54)	DM (n=25)	p
Age (mean (sd))	58.30 (10.91)	57.22 (11.45)	60.64 (9.44)	0.197
Male (%)	66 (83.5)	47 (87.0)	19 (76.0)	0.327
Multivessel PCI (%)	7 (8.9)	4 (7.4)	3 (12.0)	0.673
HTN (%)	36 (45.6)	21 (38.9)	15 (60.0)	0.094
Dyslipidemia (%)	39 (49.4)	26 (48.1)	13 (52.0)	0.812
Current smoker (%)	46 (58.2)	35 (64.8)	11 (44.0)	0.092
Culprit lesion				0.408
LAD	43(54.4)	27 (50.0)	16 (64.0)	
LCX	8(10.1)	7 (13.0)	1 (4.0)	
RCA	28(35.4)	20 (37.0)	8 (32.0)	
Baseline CMR				
LVEDV (sd) (mL)	131.17 (28.52)	131.34 (26.09)	130.77 (34.46)	0.937
LVESV (sd) (mL)	56.88 (25.50)	54.86 (20.64)	61.85 (34.79)	0.281
EF (sd) (%)	57.69 (12.17)	58.69 (10.68)	55.22 (15.25)	0.263
infarct volume (sd) (mL)	44.38 (22.53)	42.63 (21.68)	48.84 (24.64)	0.325
LV mass (sd) (mL)	117.05 (33.88)	116.76 (30.55)	117.78 (42.23)	0.914
Follow-up CMR at 6 months				
LVEDV (sd) (mL)	133.91 (35.86)	130.52 (29.16)	142.10 (48.53)	0.267
LVESV (sd) (mL)	55.54 (28.47)	50.78 (21.54)	67.03 (39.10)	0.047
EF (sd) (%)	59.83 (14.62)	61.50 (14.35)	55.81 (14.91)	0.18
Infarct volume (sd) (mL)	24.14 (9.32)	22.87 (8.73)	27.71 (10.41)	0.141
LV mass (sd) (mL)	129.34 (29.01)	127.10 (24.30)	135.66 (40.23)	0.407

Patients with DM had a higher $HbA1_C$ level at the time of myocardial infarction (7.61 ± 0.28% vs. 5.95 ± 0.11%, P <0.001). Patients with DM had lower RRU and SRU than those without DM, whereas MPRI showed no difference, as we had observed in the pig model.

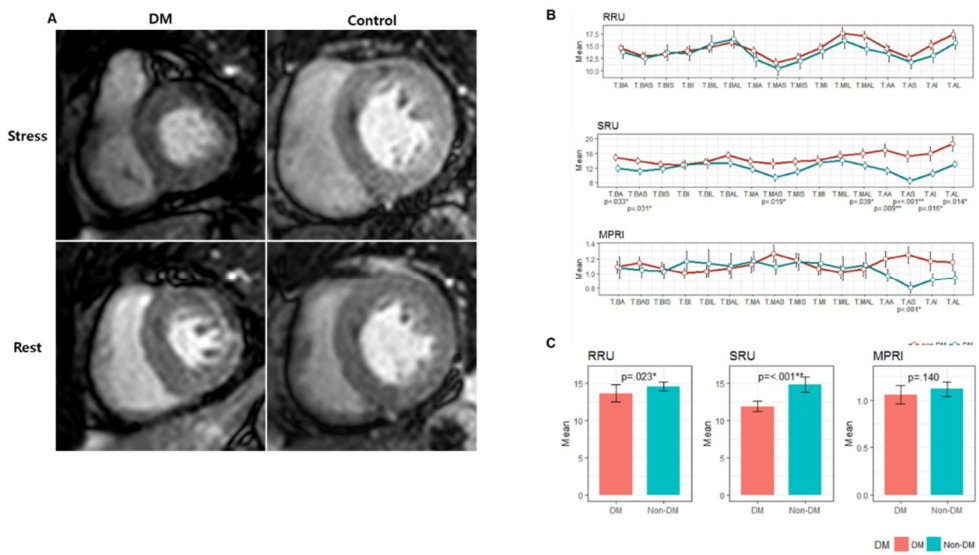

Figure 18 Representative figures of cardiac MR perfusion of diabetic and control patients

(A) MR perfusion images at stress and rest states in diabetic and control patients. (B) Mean values of the RRU, SRU and MPRI of the 16 myocardial segments. (C) Estimated mean of RRU, SRU and MPRI in diabetic and control patients.

BA = basal anterior; BAS = basal anteroseptal; BIS = basal inferoseptal; BI =

basal inferior; BIL = basal inferolateral; BAL = basal anterolateral; MA = mid anterior; MAS = mid anteroseptal; MIS = mid inferoseptal; MI = mid inferior; MIL = mid inferolateral; MAL = mid anterolateral; AA = apical anterior; AS = apical septal; AI = apical inferior; AL = apical lateral.

P value by two-way ANOVA

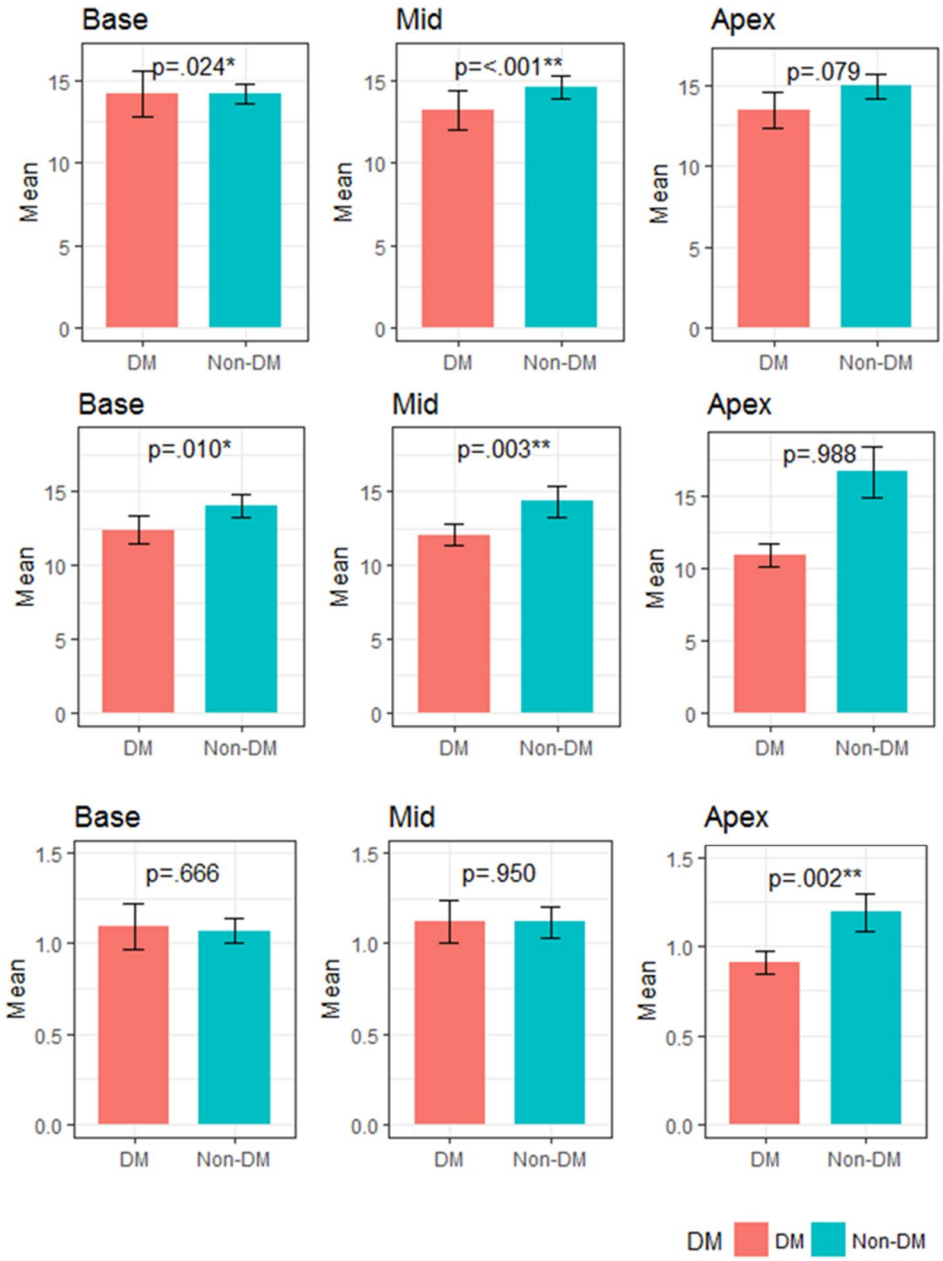

Figure 19 Myocardial perfusion of humans in CMR according to the segment location.

When stratifying the myocardial perfusion according to base, mid and apex, the MPRI in the apex was lower in diabetic patients than those without DM.

During follow-up, despite a significant decrease in $HbA1_C$, patients with DM had higher $HbA1_C$ than those without DM (6.78 ± 0.18% vs. 5.92 ± 0.09%, P < 0.001), indicating adequate DM control.

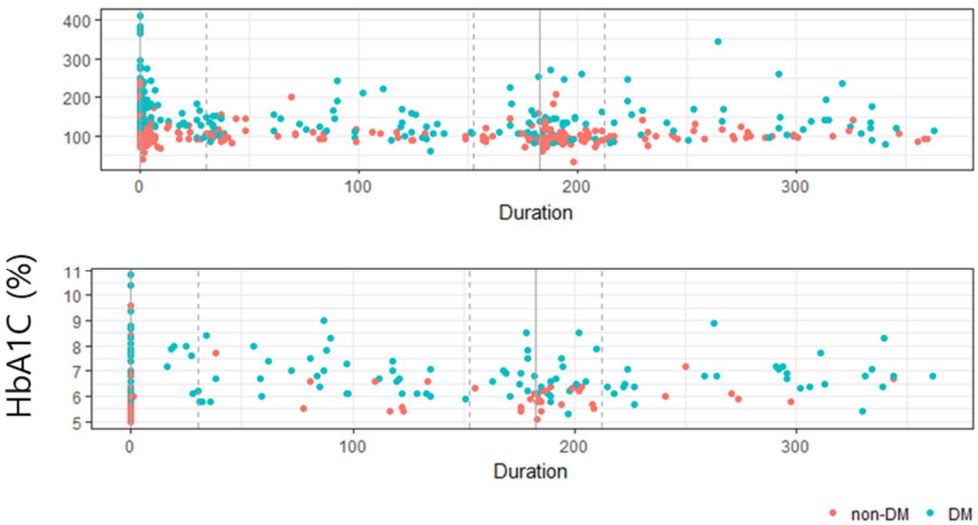

Figure 20 Blood glucose and $HbA1_C$ Diabetic patients have higher glucose and $HbA1_c$ levels.

The follow-up CMR revealed that LV end-systolic volume in patients with DM was significantly larger than that in non-DM patients (55.8 ± 14.9 ml vs.

61.5 ± 14 mL, P = 0.047). LV end-diastolic volume (142 ± 48 mL vs. 130 ± 29 mL, P = 0.267) was numerically larger and ejection fraction (55 ± 14% vs. 61 ± 14%, P =0.180) was numerically lower in DM patients than in non-DM.

Discussion

In this study, we evaluated the effect of DM on microvascular and macrovascular changes in diabetic pigs using the state-of-the-art diagnostic tools including coronary angiography, OCT, CCTA, and CMR, among others, and found the following: (i) DM caused alterations in capillary structures, (ii) without causing significant narrowing in the epicardial coronary artery during the in-vivo ex periment period, (iii) suggesting that the decreased myocardial microvascular perfusion is the result of microvascular changes. In addition, (iv) we also showed that STEMI patients with DM had decreased myocardial perfusion. To the best of our knowledge, our study is the first showing DM-related changes in microvascular structure and defects in myocardial microvascular perfusion independent of epicardial coronary artery disease in a large-animal model.

Microvascular changes and myocardial perfusion

In fluid hemodynamics, at a constant pressure, the flow is mainly determined by the resistance. Accordingly, in coronary circulation, the coronary flow will be determined by the microvascular resistance. We showed that the changes in the vessel anatomy were characterized by a smaller capillary diameter, frequent presence of acellular capillaries, and disruptions and rarefaction of the capillary. These structural changes can lead to capillary dysfunction and increase in myocardial resistance in the coronary microcirculation.

According to Hagen-Poiseuille's law for fluid hemodynamics, the resistance increases to the forth of decrease in radius.

$$R=8/\pi \times L"\eta" /(r^4)$$

R = resistance to blood flow

L = length of the vessel

η = viscosity of blood

r = radius of the blood vessel

Therefore, smaller capillary diameter alone is associated with dramatic increase in myocardial resistance. At a constant pressure, the flow is indirectly proportional to the resistance, and consequently, the flow decreases. This is also confirmed with findings from CT and MR perfusion. We repeatedly showed a decrease in myocardial perfusion by CCTA and CMR in the absence of significant epicardial stenosis. Taken together, the reduced myocardial perfusion in subjects with DM is mainly due to microvascular changes.

In humans, functional and structural abnormalities of the coronary microcirculation are often observed in diabetic patients with normal coronary arteries (12-14). The CFR is the ratio between hyperemic and resting coronary flow. In the absence of significant stenosis of the epicardial coronary arteries, the

reduction of CFR represents coronary microvascular dysfunction (15). A reduction in CFR was observed in diabetic patients without coronary artery stenosis (16). Reduction in stress myocardial blood flow and perfusion reserve has also been reported in both Type 1 and Type 2 diabetic patients in the absence of clinical coronary heart disease (25,26). The impairment of myocardial perfusion in diabetic patients may contribute to the progressive changes in cardiac function (27). This may also explain why diabetic patients are prone to development of heart failure (28) and worse outcomes after myocardial infarction compared to those without DM.

In the present study, we examined the microvascular dysfunction in the heart two months after the induction of DM. In line with our previous reports, we think that diabetic microvasculopathy progresses at an early stage of hyperglycemia due to capillary remodeling.

We could observe some discrepancies in the pattern of myocardial perfusion between pigs and humans. In pigs the relative upslope at rest, during stress, and MPRI were higher in the mid portion, whereas in humans, the apex had higher relative upslopes and MPRI. In pigs the apex of myocardium is equally supplied by posterior interventricular artery from right coronary artery (RCA) and anterior interventricular artery from left coronary artery (LCA), whereas in humans, the apex is mostly supplied by the “overwrapping LAD”. Differences in coronary anatomy may explain the discrepancies in the myocardial perfusion between pigs and humans.

Macrovascular changes

Currently, OCT is the clinically applicable imaging modality with the highest spatial resolution for the visualization of the coronary anatomy. In this study, OCT displayed no hemodynamically significant stenosis, but it did show a greater IMT in the coronary arteries of diabetic pigs. IMT represents early atherosclerotic changes of a vessel. Vascular remodeling is a homeostatic response to changes in flow and circumferential stretch to maintain or restore normal shear stress and wall (21). Theoretically, decreased coronary flow due to impaired microcirculation can lead to a decrease in vessel diameter (22) and may also accelerate atherosclerosis. Whether the increase in IMT in diabetic pigs is a result of hemodynamic alteration or a result of hyperglycemia-induced changes needs further investigation. In addition, due to the limited duration of the experiment, it is unknown whether longer exposure to hyperglycemia would have led to significant macrovascular changes as well. Nonetheless, the decrease in perfusion in the present study is not affected by the epicardial arterial changes.

Small animal, large animal, and human

We recently reported novel mechanism that abnormal intercellular signaling in endothelial cells induces microvascular rarefaction in diabetic mice(7,8). In the current study, we could reproducibly show the microvascular changes in a large

animal model. In humans, histologic examination was not feasible; however, the decreased myocardial perfusion that was observed in STEMI patients with DM, which was similar to that in diabetic pigs, implies similar microvascular changes taking place in humans. Taken together, we believe that our study provides reasonable evidence that the diabetes-induced microvasculopathy occurs in small and large animals, as well as in humans. While microvasculopathy in the animal models progressed at an early phase of hyperglycemia, the time span of microvasculopathy in humans has yet to be demonstrated. Hyperglycemia-induced capillary changes in the heart should be further investigated in the aspects of clinical significance and long-term effect on the myocardial function.

Myocardial perfusion as a clinical tool for the assessment of diabetic microvasculopathy

In our previous studies, we could reverse microvascular abnormalities by modulating the intercellular signaling, which could be a potential therapeutic target(7,8). Therefore, a non-invasive monitoring tool for the development or improvement of microvasculopathy in patients with DM is of clinical interest and is challenging. We showed that CMR showed decreased myocardial perfusion in diabetic patients, thus CMR may be a good candidate for the non-invasive assessment of microvascular changes. However, further studies with an adequate sample size are warranted before applying to clinical practice.

Clinical implications

Our study results have important clinical implications. We showed that although the pigs did not have narrowing in the epicardial coronary artery in invasive coronary angiography, they demonstrated increased intima-media thickness in OCT. Furthermore, diabetic pigs had altered capillary structure and decreased myocardial perfusion. Similarly, STEMI patients with DM had lower myocardial perfusion as well. Our study findings indicate that "normal coronary angiography results" do not mean "normal myocardial perfusion". This may also explain the clinical phenomenon of chest pain in diabetic patients with normal coronary artery.

Because the changes in microvessels occur at a very early stage, early effective interventions are mandatory.

Conclusions

DM causes increase in intima-media thickness and microvascular remodeling leading to a decrease in myocardial perfusion in large animals, which occurs at a very early stage of the disease course. Early and effective interventions are necessary to interrupt the progression of vascular complications in diabetic patients.

REFERENCES

1. Stamler J, Vaccaro O, Neaton JD, Wentworth D. Diabetes, other risk factors, and 12-yr cardiovascular mortality for men screened in the Multiple Risk Factor Intervention Trial. Diabetes Care 1993;16:434-44.
2. Haffner SM, Lehto S, Ronnemaa T, Pyorala K, Laakso M. Mortality from coronary heart disease in subjects with type 2 diabetes and in nondiabetic subjects with and without prior myocardial infarction. N Engl J Med 1998;339:229-34.
3. Carrabba N, Valenti R, Parodi G, Santoro GM, Antoniucci D. Left ventricular remodeling and heart failure in diabetic patients treated with primary angioplasty for acute myocardial infarction. Circulation 2004;110:1974-9.
4. Cooper ME, Bonnet F, Oldfield M, Jandeleit-Dahm K. Mechanisms of diabetic vasculopathy: an overview. Am J Hypertens 2001;14:475-86.
5. Jia G, DeMarco VG, Sowers JR. Insulin resistance and hyperinsulinaemia in diabetic cardiomyopathy. Nat Rev Endocrinol 2016;12:144-53.
6. Orasanu G, Plutzky J. The pathologic continuum of diabetic vascular disease. J Am Coll Cardiol 2009;53:S35-42.
7. Yoon CH, Choi YE, Cha YR et al. Diabetes-Induced Jagged1 Overexpression in Endothelial Cells Causes Retinal Capillary Regression in a Murine Model of Diabetes Mellitus: Insights Into Diabetic Retinopathy. Circulation 2016;134:233-47.

8. Yoon CH, Choi YE, Koh SJ, Choi JI, Park YB, Kim HS. High glucose-induced jagged 1 in endothelial cells disturbs notch signaling for angiogenesis: a novel mechanism of diabetic vasculopathy. J Mol Cell Cardiol 2014;69:52-66.

9. Likoff W, Segal BL, Kasparian H. Paradox of normal selective coronary arteriograms in patients considered to have unmistakable coronary heart disease. N Engl J Med 1967;276:1063-6.

10. Kemp HG, Jr. Left ventricular function in patients with the anginal syndrome and normal coronary arteriograms. Am J Cardiol 1973;32:375-6.

11. Panting JR, Gatehouse PD, Yang GZ et al. Abnormal subendocardial perfusion in cardiac syndrome X detected by cardiovascular magnetic resonance imaging. N Engl J Med 2002;346:1948-53.

12. Fein FS, Sonnenblick EH. Diabetic cardiomyopathy. Prog Cardiovasc Dis 1985;27:255-70.

13. Sunni S, Bishop SP, Kent SP, Geer JC. Diabetic cardiomyopathy. A morphological study of intramyocardial arteries. Arch Pathol Lab Med 1986;110:375-81.

14. Yarom R, Zirkin H, Stammler G, Rose AG. Human coronary microvessels in diabetes and ischaemia. Morphometric study of autopsy material. J Pathol 1992;166:265-70.

15. Dimitrow PP, Galderisi M, Rigo F. The non-invasive documentation of coronary microcirculation impairment: role of transthoracic echocardiography. Cardiovasc Ultrasound 2005;3:18.

16. Galderisi M, Capaldo B, Sidiropulos M et al. Determinants of reduction of coronary flow reserve in patients with type 2 diabetes mellitus or arterial hypertension without angiographically determined epicardial coronary stenosis. Am J Hypertens 2007;20:1283-90.

17. Yokoyama I, Momomura S, Ohtake T et al. Reduced myocardial flow reserve in non-insulin-dependent diabetes mellitus. J Am Coll Cardiol 1997;30:1472-7.

18. Quinones MJ, Hernandez-Pampaloni M, Schelbert H et al. Coronary vasomotor abnormalities in insulin-resistant individuals. Ann Intern Med 2004;140:700-8.

19. Schalkwijk CG, Stehouwer CD. Vascular complications in diabetes mellitus: the role of endothelial dysfunction. Clin Sci (Lond) 2005;109:143-59.

20. Pop-Busui R, Kirkwood I, Schmid H et al. Sympathetic dysfunction in type 1 diabetes: association with impaired myocardial blood flow reserve and diastolic dysfunction. J Am Coll Cardiol 2004;44:2368-74.

21. Langille BL. Arterial remodeling: relation to hemodynamics. Can J Physiol Pharmacol 1996;74:834-41.

22. Langille BL, O'Donnell F. Reductions in arterial diameter produced by chronic decreases in blood flow are endothelium-dependent. Science 1986;231:405-7.

23. Grussner R, Nakhleh R, Grussner A, Tomadze G, Diem P, Sutherland D. Streptozotocin-induced diabetes mellitus in pigs. Horm Metab Res

1993;25:199-203.

24. Hara H, Lin YJ, Zhu X et al. Safe induction of diabetes by high-dose streptozotocin in pigs. Pancreas 2008;36:31-8.

25. Di Carli MF, Janisse J, Grunberger G, Ager J. Role of chronic hyperglycemia in the pathogenesis of coronary microvascular dysfunction in diabetes. J Am Coll Cardiol 2003;41:1387-93.

26. Wang L, Jerosch-Herold M, Jacobs DR, Jr., Shahar E, Folsom AR. Coronary risk factors and myocardial perfusion in asymptomatic adults: the Multi-Ethnic Study of Atherosclerosis (MESA). J Am Coll Cardiol 2006;47:565-72.

27. Fonseca CG, Dissanayake AM, Doughty RN et al. Three-dimensional assessment of left ventricular systolic strain in patients with type 2 diabetes mellitus, diastolic dysfunction, and normal ejection fraction. Am J Cardiol 2004;94:1391-5.

28. Gottdiener JS, Arnold AM, Aurigemma GP et al. Predictors of congestive heart failure in the elderly: the Cardiovascular Health Study. J Am Coll Cardiol 2000;35:1628-37.

국문초록

배경

당뇨병은 관상동맥질환 발생의 위험인자이며 관상동맥질환에 동반된 경우 나쁜 예후인자로 알려져 있다. 하지만, 당뇨병이 대혈관 및 미세혈관병증을 일으키는 기전은 잘 알려져 있지 않다. 본 연구에서는 당뇨병 동물모델 돼지 및 인체에서 당뇨병이 대혈관 및 미세혈관에 미치는 영향을 밝히고자 하였다.

방법

돼지에서 당뇨병을 유발한 후 혈관조영술, 광학영상단층촬영, 심장 전산화단층촬영, 심장 자기공명영상을 시행하여 관상동맥 혈관병증 평가 및 심근 관류를 측정하였다. 실험동물은 8 주째에 안락사시키고 혈관조직을 염색하여 미세혈관병증 발생여부를 확인하였다.

결과

당뇨돼지에서 모세혈관은 불규칙한 모양이었고, 모세혈관의 내경은 대조군에 비해 유의하게 작았다 (11.7±0.33 ㎛ vs. 13.5±0.53 ㎛, P<0.001). 광학영상단층촬영에서 당뇨돼지 및 정상돼지에서 심외막

관상동맥의 협착은 관찰되지 않았다. 하지만 당뇨돼지의 내중막은 정상돼지에 비해 두꺼웠다. 심장 자기공명영상에서 당뇨돼지는 휴식 (31.3±5.9 vs. 37.9±8.1, P = 0.011) 및 스트레스시 (18.0±3.0 vs. 21.6±2.8, P = 0.007) 상대적 경사도(relative upslope)가 유의하게 낮았는데, 이는 당뇨돼지의 심근 관류가 정상돼지에 비해 저하되어 있다는 것을 시사한다.

한편, 79 명의 ST 분절상승 심근경색으로 치료를 받은 환자 중에 25 명이 당뇨병을 갖고 있었다. 심장 자기공명영상에서 당뇨병이 있는 환자가 당뇨병이 없는 환자에 비해서 심근관류가 저하되어 있었다.

결론

당뇨병은 대동물에서 조기에 미세혈관병증 및 심근 관류의 저하를 일으킨다. 당뇨병 초기에 혈당 조절 등의 치료를 철저히 한다면 당뇨병으로 인한 혈관 합병증의 진행을 막고 심혈관계 합병증을 예방할 수 있을 것으로 기대한다.

학번: 2011-30599